BBA - Bioenergetics 1862 (2021) 148332

Contents lists available at ScienceDirect

BBA - Bioenergetics

journal homepage: www.elsevier.com/locate/bbabio

Digitonin concentration is determinant for mitochondrial supercomplexes analysis by BlueNative page

Sara Cogliati [a,b,*], Fernando Herranz [c,d], Jesús Ruiz-Cabello [d,e,f,g], José Antonio Enríquez [a,h,**]

[a] Centro Nacional de Investigaciones Cardiovasculares Carlos III (CNIC), Melchor Fernández Almagro, 3, 28029 Madrid, Spain
[b] Departamento de Biología Molecular, Centro de Biología Molecular Severo Ochoa, Consejo Superior de Investigaciones Científicas-Universidad Autónoma de Madrid (CSIC-UAM), Madrid, Spain
[c] NanoMedMol, Instituto de Química Médica, Consejo Superior de Investigaciones Científicas (IQM-CSIC), 28006 Madrid, Spain
[d] CIBER de Enfermedades Respiratorias (CIBERES), 28029 Madrid, Spain
[e] Center for Cooperative Research in Biomaterials (CIC biomaGUNE, 2014), Basque Research and Technology Alliance (BRTA), Paseo de Miramon 182, 20014, Donostia-San Sebastián, Spain
[f] IKERBASQUE, Basque Foundation for Science, Bilbao, Spain
[g] Facultad de Farmacia, Universidad Complutense de Madrid, 28040 Madrid, Spain
[h] CIBERFES, Madrid, Spain

ARTICLE INFO

Keywords:
BlueNative page
Mitochondria
Supercomplexes
Digitonin
Detergent
Liquid dispersions

ABSTRACT

The BlueNative page (BNGE) gel has been the reference technique for studying the electron transport chain organization since it was established 20 years ago. Although the migration of supercomplexes has been demonstrated being real, there are still several concerns about its ability to reveal genuine interactions between respiratory complexes. Moreover, the use of different solubilization conditions generates conflicting interpretations. Here, we thoroughly compare the impact of different digitonin concentrations on the liquid dispersions' physical properties and correlate with the respiratory complexes' migration pattern and supercomplexes. Our results demonstrate that digitonin concentration generates liquid dispersions with specific size and variability critical to distinguish between a real association of complexes from being trapped in the same micelle.

1. Introduction

The BlueNative page (BNGE), together with the cryo-electron microscopy, is the most useful technique to study the organization of the respiratory chain complexes (RCs) and supercomplexes (SCs). It was set up 20 years ago already by Hermann Schägger, who used this technique to study the structure of bovine and yeast SCs [1,2], and since then, its use has been spreading in the field [3,4]. It allows the isolation of protein complexes by mitochondrial membrane solubilization with a mild anionic detergent, such as digitonin. After adding a Coomassie dye, that confers a negative charge, the protein complexes can migrate in a polyacrylamide gradient gel. In these native conditions, the protein complexes maintain their physiological interactions that allow structural studies [5]. Besides, they preserve their enzymatic activities that could be detected either by specific in-gel assays [6], by respirometry [5,7]or by spectrophotometry [5].

BNGE allowed the description of mitochondrial SCs [1] and corroborated the *plasticity model* [7]. However, due to the use of detergents (mainly digitonin), it has suffered many criticisms. The most evident was the consideration of SCs as artifacts resulting from digitonin solubilization of the mitochondrial membranes. Later, the identification of SCs in different species [8–14], genetic modulation of complex subunits [7,15], the use of detergent-free methods [7,16,17], the discovery of the assembly factors [18–20]and their visualization on cryo-electron microscopy [21–24]definitively demonstrate the existence of SCs. However, there are still some concerns about the use and the consequent interpretation of BNGE, mainly due to not homogenous use of digitonin concentration: (i) some authors consider all the free CI as an artifact of the technique due to the action of detergent [1,25]; (ii) all co-migrations are interpreted as evidence of interactions between protein complexes

* Correspondence to: S. Cogliati, Departamento de Biología Molecular, Centro de Biología Molecular Severo Ochoa, Consejo Superior de Investigaciones Científicas-Universidad Autónoma de Madrid (CSIC-UAM), Calle Nicolás Cabrera, 1, 28049, Madrid, Spain.
** Correspondence to: J.A. Enríquez, Centro Nacional de Investigaciones Cardiovasculares Carlos III (CNIC), Melchor Fernández Almagro, 3, 28029 Madrid, Spain.
E-mail addresses: sara.cogliati@uam.es (S. Cogliati), jaenriquez@cnic.es (J.A. Enríquez).

https://doi.org/10.1016/j.bbabio.2020.148332
Received 30 August 2020; Received in revised form 9 October 2020; Accepted 26 October 2020
Available online 28 October 2020

disregarding if the molecular mass is or not compatible with the migration position; (iii) the contribution of the lipid composition to the migration is ignored; (iv) several migration positions are systematically ignored despite being persistent; (v) the actual proportion of solubilized respiratory complexes among the total population present in the sample is not systematically estimated. All these issues may hamper the interpretation of the BNGE studies adding confusion to the field. For example, in heart and muscle mitochondria, there are different bands defined as SCs I + III_2 + IV (also called N-respirosome) [5] that has been explained as due to an increasing amount of CIV monomers (1–4) [2] without sufficient experimental support. In the BNGE, solubilization conditions are fundamental for ensuring proper dispersion while maintaining SCs interaction. In particular the optimal ratio detergent/protein has been set up carefully by Schägger [1,3], showing that it should be adjusted accordingly to the species [3,26], but these rules are not universally followed.

In this work, we study the effects of different digitonin concentration on BNGE, demonstrating that below 1 g digitonin/1 g mitochondria (g_{DIG}/g_{MITO}), RCs and SCs migrate as a bulk of undefined bands. Starting with 2 g_{DIG}/g_{MITO}, discrete bands positive for CI, II, III and IV appear but only with higher concentration could the bigger SCs be defined. Moreover, we demonstrate that the multiple bands positive for CIV only in heart mitochondria [19] are stable also at high detergent concentrations (up to 20 g_{DIG}/g_{MITO}), revealing a strong interaction that eventually calls for further analysis. In the original work by Schägger, 4 g_{DIG}/g_{MITO} has been used [1] for mammalian mitochondria, and our data confirm that not only can it define specific and real interactions, but it can fully extract most of the mitochondrial protein content. Finally, using dynamic light scattering (DLS) we determine that digitonin concentration is inversely correlated with mean liquid dispersions diameter and directly correlated with heterogeneity in population size mirroring the migration profiles on BNGE.

2. Material and methods

2.1. Mitochondria isolation

Mitochondria from liver and heart were isolated according to the previously described method [27] and the mitochondrial protein amount was quantified by Bradford assay (Bio-Rad, 5000006).

2.2. Mitochondrial membrane solubilization

To detect respiratory chain complexes and supercomplexes, mitochondria from mouse heart and liver were suspended at 10 mg protein/ml in an appropriate volume of 50 mM Imidazole, 500 mM 6-aminohexanoic acid, EDTA 1 mM pH 7. They were then solubilized 5 min in ice with the indicated amount of digitonin (50% TLC, from Sigma (D5628), solubilized in Imidazole 50 mM, 6-aminohexanoic acid 500 mM, EDTA 1 mM not recrystallized). Following centrifugation in an Eppendorf centrifuge 5415R at 16,000 ×*g* for 20 min, at 4 °C the supernatant was collected and Serva Blue G dye (Serva Scientist), stock 5% was added at the ratio detergent/dye of 8.

2.3. BNGE electrophoresis

Samples were separated in non-denaturing conditions on a 3–12% gradient gel as previously described [3]. The gradient gels were prepared into Biorad Mini protein 1,5 mm system using a peristaltic pump.

2.4. Immunoblots

After electrophoresis, gels were electroblotted onto Hybond-P-polyvinylidene fluoride (PVDF) membranes (GE Healthcare) and immunoblotted with specific antibodies against the different subunits of the complexes (anti-COX1, Invitrogen; anti-core2 Protein Tech; anti-NDUFS5 Protein Tech; anti-Fp70 Invitrogene). The secondary antibodies were conjugated to LI-COR IRDye 800 CW or 680 LT (Rockland antibodies) and acquired with the ODYSSEY Infrared Imaging System (LI-COR) except for anti-Fp70 that was revealed by ECL detection reagent (Amersham) with secondary antibody conjugated to HRP.

2.5. Transmission electron microscopy

TEM images were obtained with a JEOL JEM 1010 machine operated at 100 kV. Triplicate samples were dropped onto a formvar-coated TEM grid, air-dried and then stained with 2% ammonium molybdate solution. The grid was air dried before TEM measurements.

2.6. Dynamic light scattering

Hydrodynamic size and polydispersity index of liquid dispersions in digitonin solubilized fresh mitochondrial preparations were measured with a Zetasizer Nano ZS90 instrument equipped with a 633 nm He-Ne laser. Samples were equilibrated at room temperature and measured three times without previous treatment in disposable 40 μl cells. All samples were studied by cumulant analysis to determine the Z-average and intensity profile of the scattered light. Volume distributions were obtained by the use of Mie theory with the instrument software.

2.7. Animal strains

Parental C57BL/6JOlaHsd and CD1 strains were purchased from Harlan Laboratories and the colonies was maintained in-house animal facility. All animal procedures conformed to EU Directive 86/609/EEC and Recommendation 2007/526/EC regarding the protection of animals used for experimental and other scientific purposes, enforced in Spanish law under Real Decreto 1201/2005.

3. Results

3.1. Different concentrations of digitonin produce substantial differences in the migration pattern of mitochondrial complexes and supercomplexes

To understand how digitonin concentration could affect the BNGE migration of mitochondrial proteins, we analyzed the effect of increasing digitonin concentration (0–10 g_{DIG}/g_{MITO}) on BNGE comparing mitochondrial preparation from CD1 and C57Bl/6J(BL6) harboring the functional form (113 aa) or the mutated form (111 aa) respectively of the supercomplexes assembly factor 1 (SCAF1/COX7A2L) [18,19]. SCAF1mediates the interaction between CIII with IV that is lost in BL6 animals, therefore comparing both samples could allow us to better track the impact of solubilization of SCs migration. To do that, we first monitored the migration of CIV since it migrates in multiple bands in BNGE: as IV_{1-2}, Q-respirasome [5] (III_2 + IV_{1-2}), I + IV_{1-2}, N-respirasome (I + III_2 + IV_{1-2}). Then we confirmed the results by monitoring the migration of CI and CIII.

At digitonin concentrations < 0.5 g_{DIG}/g_{MITO}, no CIV is detected, at 0.5 g_{DIG}/g_{MITO} all CIV migrates as high molecular weight entities, and at 1 g/g multiple discrete bands are positive for CIV (Fig. 1A, left panels). No differences in CIV migration patterns were observed between CD1, and BL6 derived samples at digitonin concentrations ≤0.5 g_{DIG}/g_{MITO}. At higher digitonin concentrations, the two samples revealed conspicuous differences. In sample CD1, four major bands positive for CIV are stably detected between 2 and 10 g_{DIG}/g_{MITO}: The N-respirasome, the Q-respirasome, dimer, and monomer CIV (Fig. 1A left, upper panel). In contrast, with increasing digitonin concentration, the BL6sample progressively loses all CIV-positive bands except the two fastest-migrating bands, corresponding to monomeric and dimeric CIV (Fig. 1A left, down panel). CI does not migrate as discrete bands up to 1–2 g_{DIG}/g_{MITO}, where it appears with $CIII_2$ and only in CD1 mitochondria forming the N-respirasome (I + III_2 + IV) (Fig. 1A middle panels). Below 0.5 $g_{DIG}/$

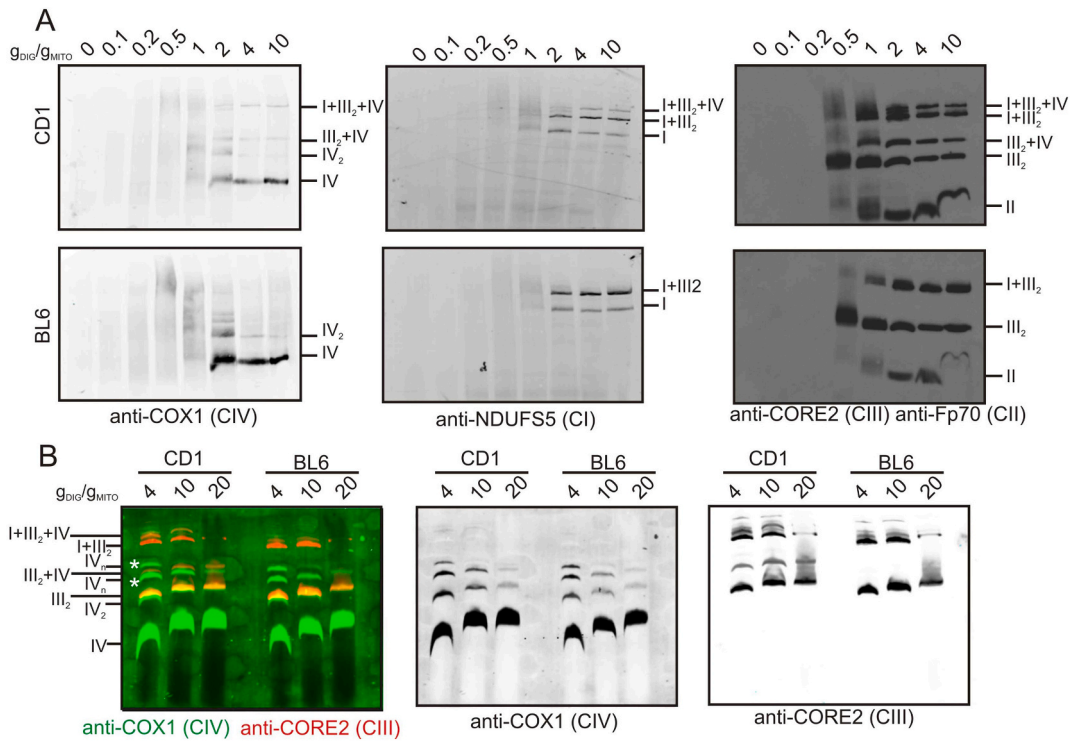

Fig. 1. Effect of different digitonin concentration on complexes and supercomplexes migration patterns. (A) BNGE immunoblots of (A) liver and (B) heart mitochondrial samples from the indicated mouse strains after solubilization at different digitonin concentrations.

g_{MITO}, CIII predominantly migrates as a bulk of dimer plus one blur upper band in BL6 and two in CD1 resembling its association with CIV (Fig. 1A left panel). From 2 g_{DIG}/g_{MITO}, in both mouse strains, $CIII_2$ and SCI + III_2 migrate as defined bands but only in CD1 interaction with CIV within the N- and Q-respirasomes is observed. Starting from 1 g_{DIG}/g_{MITO}, CII is detected as a monomer at the lowest part of the gel although higher digitonin concentrations interfere with its electrophoretic migration (Fig. 1A left panel). The results demonstrate that the digitonin concentration is critical for RCs and SCs bands definition and that CIV positive bands show the most variability upon different digitonin concentration. We have previously shown that, upon 4 g_{DIG}/g_{MITO}, heart mitochondria show a characteristic pattern of bands positive for CIV specific to adult heart [19] (Fig. 1B left panel, white asterisk). In order to exclude that these new bands were artifacts due to the incomplete solubilization of heart mitochondrial membranes, we compare the separation pattern of higher digitonin concentration in BL6 and CD1 heart mitochondria. The results show that up to 10 g_{DIG}/g_{MITO}, all the bands positive for CIV and $CIII_2$ are presently being the Q-respirasome (III_2 + IV) only detectable in CD1 mitochondria (Fig. 1B). At 20 g_{DIG}/g_{MITO}, the low migrating bands of SCs are compromised, and the overall migration pattern is altered. The results confirm that the multimers of CIV of heart mitochondria are specific and stable even at stronger solubilization conditions. Thus, the standard digitonin concentration 4 g_{DIG}/g_{MITO}, used for protein-rich mammalian mitochondria by Schägger [1] is the lowest that allows the separation of discrete bands which remain stable even at higher digitonin concentration without interfering with their electrophoretic migration. It is important to notice that in a later work, the amount of digitonin used for mammalian mitochondria was 6 g_{DIG}/g_{MITO} [3]. However, since our results show that the migration pattern do not essentially change between 4 and 10 g_{DIG}/g_{MITO}, we consider 4 g_{DIG}/g_{MITO} as the standard conditions for mammalian mitochondria.

3.2. 4 g_{DIG}/g_{MITO} is sufficient to extract all mitochondrial electron transport chain proteins

To further assess whether the amount of mitochondrial proteins extracted with 4 g_{DIG}/g_{MITO} represents the total amount, we performed serial solubilization of heart mitochondrial preparations with an increasing amount of digitonin (Fig. 2). The first solubilization shoot with 4 g_{DIG}/g_{MITO} was able to extract all the structures containing CIV in both BL6 and CD1 mitochondria except for a minority number of CIV monomer and dimers extracted with additional solubilization of the mitochondria pellet with 10 g_{DIG}/g_{MITO}. A residual amount of CIV monomer was extracted, adding 20 g_{DIG}/g_{MITO} of digitonin (Fig. 2 right panel in green, middle panel). CIII dimer and in association with CI was extracted entirely with 4 g_{DIG}/g_{MITO} in both mitochondrial strains (Fig. 2 left panel, red signal, and left panel), but associated with CIV only in CD1 (Fig. 2 yellow signal). No additional amount is extracted with an increasing amount of digitonin. The results confirm that 4 g_{DIG}/g_{MITO} of digitonin is sufficient to essentially extract the total amount of RC and SCs, preserving the differences between the two mouse strain mitochondria.

3.3. Solubilization in less than 4 g_{DIG}/g_{MITO} produces bigger liquid dispersions that can trap complexes that do not interact

We examined the effect of digitonin concentration by dynamic light scattering (DLS; photon correlation spectroscopy) in mitochondrial samples (CD1 background). This technique allows the determination of small particles' size distribution profile (like liposomes or liquid dispersions) in suspension. As expected, digitonin concentration inversely correlates with mean liquid dispersions diameter, which was substantially smaller at 4 g_{DIG}/g_{MITO} than at 1 g_{DIG}/g_{MITO} (Fig. 3A, black bars). Another relevant parameter is the polydispersity index (PdI), a dimensionless measure of the difference between the largest and the smallest measurable liquid dispersions in the sample; the higher the Pdl, the larger this difference (for the Zetasizer NanoZS90 instrument used here

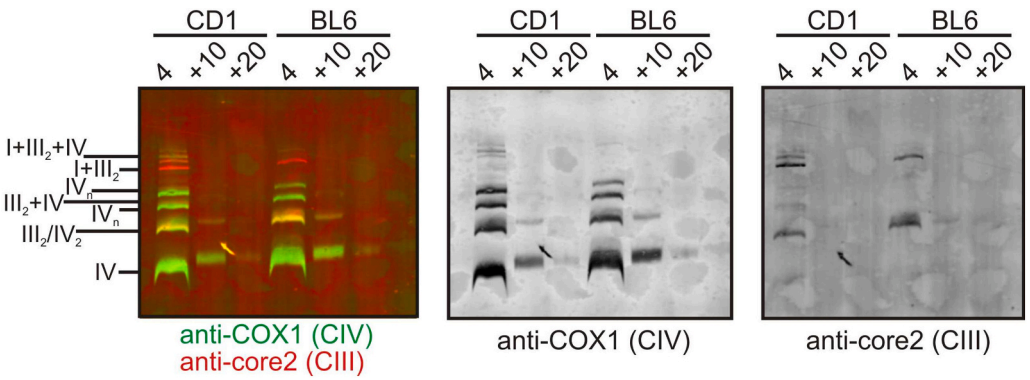

Fig. 2. Mitochondrial solubilization with increasing digitonin concentration.
BNGE immunoblots of heart mitochondrial samples of the indicated mouse strains. Mitochondria were first solubilized with 4 g_{DIG}/g_{MITO} of digitonin and the remaining pellet with further 10 g_{DIG}/g_{MITO} and 20 g_{DIG}/g_{MITO}.

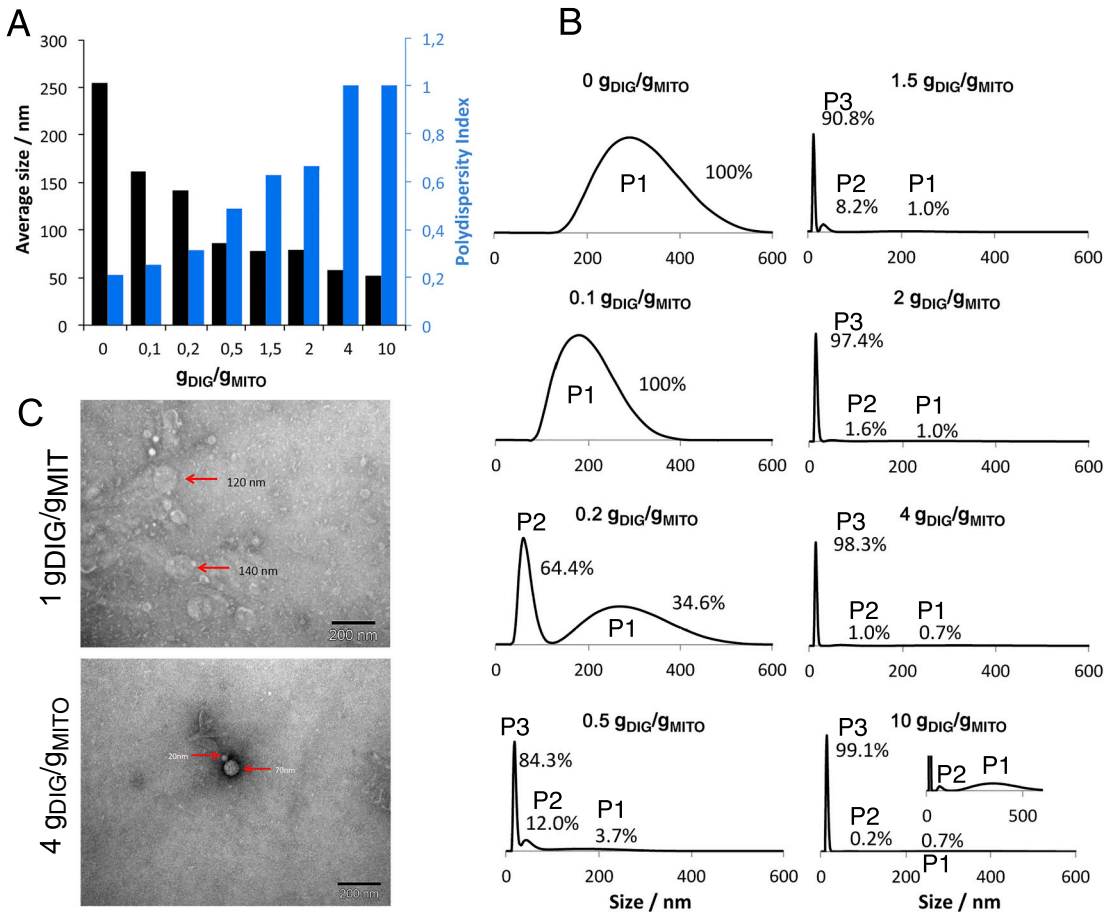

Fig. 3. Dynamic light scattering (DLS) and transmission electron microscopy (TEM) analysis of digitonized mitochondrial samples (A) Effect of digitonin concentration on the mean diameter of liquid dispersions in suspension (average size, black) and on the polydispersity index (blue). (B) Effect of digitonin concentration on liquid dispersions size in mitochondrial preparations. Liquid dispersions population 1 (P1), mean diameter ~300 nm; P2, ~60 nm; P3, ~14 nm. (C) Representative TEM images confirm that samples at 1 g/g contain more large liquid dispersions and membrane fragments than samples at 4 g_{DIG}/g_{MITO}, but even at the higher concentration, large liquid dispersions are easily detected. (For interpretation of the references to color in this figure legend, the reader is referred to the web version of this article.)

the value is always between 0 and 1). PdI increased with increasing Digitonin concentration over the range tested (Fig. 3A, blue bars), mirroring the Z-average concentration-dependent decrease. This analysis indicates: 1) although liquid dispersions diameter decreases progressively with increasing digitonin concentration, even at high concentrations larger particles are not eliminated; 2) from 1 g_{DIG}/g_{MITO} to 4 g_{DIG}/g_{MITO}, PdI increases substantially, indicating a corresponding drop in the size of the smallest measurable liquid dispersions; in other words, the smallest liquid dispersions are bigger at 1 g_{DIG}/g_{MITO} than at 4 g_{DIG}/g_{MITO}; 3) at high concentration the population of liquid dispersions has more variability being able so to embed protein complexes of different size. A dynamic picture of what is going on can be obtained by estimating the heterogeneity in population size and each population's contribution to the size average and PdI. The plots in Fig. 3B show the

percentage distribution of particle size at different digitonin concentrations. For simplicity, we consider three major populations of average diameter of 300 nm (P1), 60 nm (P2), and 14 nm (P3). In the absence of detergent, a single population of large liquid dispersions corresponds to intact mitochondria (P1), and this population shifts to a smaller size at 0.1 g_{DIG}/g_{MITO} but is not disrupted. At 0.2 g_{DIG}/g_{MITO}, the homogenous population splits into populations P1 and P2. P3 appears at 0.5 g_{DIG}/g_{MITO}, and though all three populations are present at this concentration, most vesicles are P3, explaining why average diameter decreases as PdI increases. P1 and P2 populations decrease further in favor of P3 from 0.5 g_{DIG}/g_{MITO} to 1 g_{DIG}/g_{MITO}, but significant proportions of P2 and P1 remain, as verified in TEM images (Fig. 3C). At 2 g_{DIG}/g_{MITO}, the P3 notably increases, reaching nearly 100% at 10 g_{DIG}/g_{MITO}, however, P1 and P2 are still present and detectable in TEM images (Fig. 3C).

Thus, the DLS and TEM analysis yield three major conclusions: (1) Increasing the concentration of digitonin first induces a transient population of large liquid dispersions (P1 and P2) that are progressively transformed into a population of small liquid dispersions. (2) At 0.1 g_{DIG}/g_{MITO}, the contribution of the population of transient and heterogeneous liquid dispersions is very relevant, and the liquid dispersions of minimum size are not achieved. Therefore, the likelihood of trap respiratory complexes in large liquid dispersions is more significant than at 4 g_{DIG}/g_{MITO}. Thus, correlating the DLS results with the BNGE migration patterns (Fig. 1), we can conclude that the appearance of P3 population is determinant for the isolation of smaller bands in the BNGE and that the variability of the liquid dispersions is fundamental to trap different multimerization complexes. On the contrary, the migration in a unique upper bulk at low digitonin concentration 0.5 g_{DIG}/g_{MITO} could be due to big particles' single population.

4. Discussion

The electron transport chain (ETC) organization has been at the center of a passionate debate since the conception of the fluid [28] and solid model [29] further integrated into the plasticity model [7]. It is widely accepted that the ETC complexes coexist in their monomeric states and assembled into bigger associations called SCs [4,30,31]; but, how many SCs do exist and what are their composition are still unsolved issues. Moreover, understanding whether SCs have specific bioenergetic functions and their physiological impact is almost unknown [5,31].

For that, the field needs a trustable technique with a clear consensus. BNGE is considered the golden technique to study the ETC organization and SCs composition according to the electrophoretic migration profile. Despite 20 years of experimentation, the discussions on the ability of BNGE to reveal genuine interactions between respiratory complexes have produced strong warnings and caveats. The use of detergent for the solubilization of membrane components is the major criticism of BNGE, and for that, SCs have been considered artifacts since genetic and detergent-free approaches finally demonstrated them.

The question on the solubilization conditions has been an old and central issue already addressed by different authors [1,3,32]. Despite the clear and concrete indications of the original works of Schägger [1,3] still, there is variability in the handling of technique that could lead to misunderstanding and generate more noise in the field. In this work, we address the effects of digitonin's different concentrations on the mitochondrial proteins profile patterns and characterize the physical properties of the resulting liquid dispersions by DLS to determine the most reliable solubilization condition. Our experiments demonstrated that a proper migration correlates with the detergent-forming liquid dispersions with a less average diameter and more size variability defined as polydispersity index. The critical concentration is 1 g_{DIG}/g_{MITO}, where the bigger liquid dispersions, P2, P1, are dramatically reduced in favor of the P3 smaller liquid dispersions, which became even more predominant at 2 g_{DIG}/g_{MITO} and 4 g_{DIG}/g_{MITO}. The physical changes of liquid dispersions correlate with the appearance of discrete bands at the correspondent molecular weight of RC and SCs, which became more defined by losing the blur signal meaning of uncomplete mitochondrial membrane solubilization. One of the standard concentrations defined by Schägger for mammalian mitochondria is 4 g_{DIG}/g_{MITO} [1], and we show here that this concentration allows extracting all mitochondrial inner membrane proteins and defines correct SCs interactions that are stable even at higher digitonin concentrations. It means that this concentration is the most reliable to characterize ETC organization in mammalian mitochondria minimizing the risk of artifacts.

Our analysis reveals that solubilization of membrane components with detergents generates liquid dispersions that can trap complexes, giving the impression of physical interaction when they are merely in the same vesicular structure. This real risk could be lessened by using the correct amount of digitonin. Indeed, our results demonstrated that digitonin's low concentration could produce more artifacts and substantial variations than high concentration. Mitochondria from different species and tissues could also differ in phospholipid and protein composition that could interfere with proper membrane solubilization. For that, it would be beneficial testing the sample/detergent ratio in the specific mitochondria type to be studied.

The inability to eliminate larger liquid dispersions underlines the need for rigor in the interpretation of BNGE results. Even with the right detergent proportion, it is hard to determine if low-abundance bands represent biologically-relevant protein associations or incompletely solubilized membrane proteins incorporated into the larger liquid dispersions. This limit could be reason why we still do not know if complex II superassembles. Since we only find minute amounts of CII co-migrating with other complexes [7], we cannot exclude the possibility that this is an artifact due to large remnant liquid dispersions in the preparation.

The migration of CI as a single complex still generates some concerns. Our results show that CI appears as a monomer with 1 g_{DIG}/g_{MITO} without significantly increasing its proportion up to 10 g_{DIG}/g_{MITO}. Moreover, other publications demonstrated that mitochondrial from some species [26], included human muscle mitochondria [33], do not show any detectable band with CI alone, suggesting that it is more probably due to the specific ETC organization than to digitonin. The physiological meaning of having or not a proportion of free CI remains unknown. The formation of the N- and Q-respirasomes depends on SCAF1 [5]. The use of non-homogeneous BNGE may, however, originate contradictory results. Thus, at intermediate concentrations of digitonin (1–2 g_{DIG}/g_{MITO}) the liver mitochondrial samples harboring functional or non-functional SCAF1 showed a pattern of CIV bands that may be interpreted as revealing the presence of N- and Q-respirasomes (Fig. 1A). The migration pattern of CIII indicates that the CIV migrating in this area is not associated with III_2in the absence of functional SCAF1, and therefore could not represent a respirasome. Thus, at higher concentration of digitonin only SCAF1 positive samples reveals CIV in high molecular SCs, eliminating any risk of misinterpretation. In the heart mitochondria, we found extra-bands positive for CIV [5] resistant at high digitonin concentrations (up to 10 g_{DIG}/g_{MITO}). The reasons for their different profile migrations, their specificity for heart mitochondrial, and their physiological role are still unknown, but their migrations very close to some SCs may lead to the wrong impression that they represent forms of the Q-respirasome ($III_2 + IV$ or $III_2 + IV_2$). This issue is particularly problematic when using small gels or short running times. It is important to mention that in the absence of SCAF1, the Q-respirasome is absent in heart mitochondria. However, a low level of N-respirasome can be observed (Fig. 1B). We recently demonstrated that the SCAF1 deficient N-respirosome is functionally and structurally different from the wild type one [5] being determined by the independent interaction of CI with $CIII_2$ and with CIV, even though the interaction between $CIII_2$ and CIV is lost [5]. This respirosome results more sensitive to stronger solubilization conditions as observed independently by us [5] (using second dimension DDM BNGE) and by other authors [32] (using increasing amount of digitonin). In this context, the digitonin/

protein ratio could be considered as an indicator of the stability of supercomplexes [34].

It is worth to notice, that also the timing and the temperature conditions of sample handling could be determinant. Inspired by the observation that respirosome shift from tight to loose conformation upon delayed grid preparation [21], we extensively study the stability of respirosome upon over-night incubation at 4C and demonstrated that in solubilized mitochondrial preparation, the CIII+IV interaction within the respirosome is lost due to the proteolytic processing of SCAF1 [5]. Therefore, we concluded that the sample handling as storage temperature and timing is relevant for the study of the SCs organization as already hypothesized by others [34].

Despite the concerns and limitations, the BNGE technique remains the most used and useful technique to study ETC, and for that, it is crucial to be aware of the limitations and minimize the possibility of artifacts. Here, we point out the importance of solubilization conditions, and we warn against the possible pitfalls. However, it would always be beneficial to corroborate the BNGE results with complementary techniques such as second dimension BNGE, proteomics, or genetics approach. Looking at the emerging physiological relevance of the ETC organization [5,33,35–39], we guess that soon, it would be fundamental improving in situ techniques such as cryo-electron tomography [40,41] and stimulated emission depletion microscopy (STED) [42] [43], to study the ETC organization without isolating RCs and SC, along with the already on-going techniques for tracking the formation of SCs [44–46].

5. Conclusion

Digitonin concentration is fundamental for the proper mitochondrial solubilization that depends on the detergent-forming liquid dispersions dispersion. In particular, we demonstrated that the average size and the heterogeneity of liquid dispersions (expressed as polydispersity) are the determinants for the protein complexes separation on BNGE. However, we detected large detergent vesicles that could trap uncomplete solubilized membrane proteins at high digitonin concentration, which could generate artifacts. For that, it would be fundamental to set the proper digitonin:sample ratio, carefully analyze the BNGE results and confirm it with complementary techniques.

Declaration of competing interest

The authors declare that they have no known competing financial interests or personal relationships that could have appeared to influence the work reported in this paper.

Acknowledgment

S.C. is recipient of “Ramon y Cajal” fellowship (RyC-2017-23013).

The CNIC is supported by the Ministry of Economy, Industry and Competitiveness (MEIC) and the Pro-CNIC Foundation and is a Severo Ochoa Center of Excellence (MINECO award SEV-2015-0505). Work in the laboratory of J.A.E. is funded by the CNIC and a grant by Ministerio de Ciencia, Innovación e Universidades (MICINN), Agencia Estatal de Investigación (AEI) and Fondo Europeo de Desarrollo Regional (FEDER; SAF2015-65633-R & RTI2018-099357-B-I00), the Biomedical Research Networking Center on Frailty and Healthy Ageing (CIBERFES-ISCiii) and the HFSP agency (RGP0016/2018). CIC biomaGUNE is supported by the Maria de Maeztu Units of Excellence Program from the Spanish State Research Agency – Grant No. MDM-2017-0720. JRC acknowledges grants from MEIC (SAF2017-84494-C2-R), the Gobierno Vasco - Dpto. Industria, Innovación, Comercio y Turismo-ELKARTEK Program (Grant No. KK-2019/bmG19) and a grant from the BBVA Foundation.

References

[1] H. Schagger, K. Pfeiffer, Supercomplexes in the respiratory chains of yeast and mammalian mitochondria, EMBO J. 19 (2000) 1777–1783.
[2] H. Schägger, K. Pfeiffer, The ratio of oxidative phosphorylation complexes I-V in bovine heart mitochondria and the composition of respiratory chain supercomplexes, J. Biol. Chem. 276 (2001) 37861–37867.
[3] I. Wittig, H.-P. Braun, H. Schägger, Blue native PAGE, Nat. Protoc. 1 (2006) 418–428.
[4] J. Enríquez, A. Supramolecular, Organization of respiratory complexes, Annu. Rev. Physiol. 78 (2016) 533–561.
[5] Calvo, E. et al. Functional role of respiratory supercomplexes in mice: SCAF1 relevance and segmentation of the Q pool. Sci. Adv. 6, eaba7509 (2020).
[6] I. Wittig, M. Karas, H. Schägger, High resolution clear native electrophoresis for in-gel functional assays and fluorescence studies of membrane protein complexes, Mol. Cell. Proteomics 6 (2007) 1215–1225.
[7] R. Acín-Pérez, P. Fernández-Silva, M.L. Peleato, A. Pérez-Martos, J.A. Enriquez, Respiratory active mitochondrial supercomplexes, Mol. Cell. 32 (2008) 529–539.
[8] I. Marques, N.A. Dencher, A. Videira, F. Krause, Supramolecular organization of the respiratory chain in Neurospora crassa mitochondria, Eukaryot. Cell 6 (2007) 2391–2405.
[9] F. Krause, et al., ‘Respirasome’-like supercomplexes in green leaf mitochondria of spinach, J. Biol. Chem. 279 (2004) 48369–48375.
[10] H. Eubel, L. Jansch, H. Braun, New insights into the respiratory chain of plant mitochondria. Supercomplexes and a unique composition of complex II, Plant Physiol. 133 (2003) 274–286.
[11] García-Poyatos, C. et al. Scaf1 promotes respiratory supercomplexes and metabolic efficiency in zebrafish. EMBO Rep. 1–20 (2020) doi:10.15252/embr.202050287.
[12] Y. Arribat, et al., Mitochondria in embryogenesis: an organellogenesis perspective, Front. Cell. Dev. Biol. 7 (282) (2019).
[13] I. Llorente-Garcia, et al., Single-molecule in vivo imaging of bacterial respiratory complexes indicates delocalized oxidative phosphorylation, Biochim. Biophys. Acta Bioenerg. 1837 (2014) 811–824.
[14] A. Stroh, et al., Assembly of respiratory complexes I, III, and IV into NADH oxidase supercomplex stabilizes complex I in Paracoccus denitrificans, J. Biol. Chem. 279 (2004) 5000–5007.
[15] R. Acín-Pérez, et al., Respiratory complex III is required to maintain complex I in mammalian mitochondria, Mol. Cell 13 (2004) 805–815.
[16] T. Althoff, D.J. Mills, J.-L. Popot, W. Kühlbrandt, Arrangement of electron transport chain components in bovine mitochondrial supercomplex I_1 III_2 IV_1, EMBO J. 30 (2011) 4652–4664.
[17] N.V. Dudkina, H. Eubel, W. Keegstra, E.J. Boekema, H.-P. Braun, Structure of a mitochondrial supercomplex formed by respiratory-chain complexes I and III, Proc. Natl. Acad. Sci. 102 (2005) 3225–3229.
[18] Lapuente-Brun, E. et al. Supercomplex assembly determines electron flux in the mitochondrial electron transport chain. Science (80-.). 340, 1567–1570 (2013).
[19] S. Cogliati, et al., Mechanism of super-assembly of respiratory complexes III and IV, Nature 539 (2016) 579–582.
[20] K.M. Hatle, et al., MCJ/DnaJC15, an endogenous mitochondrial repressor of the respiratory chain that controls metabolic alterations, Mol. Cell. Biol. 33 (2013) 2302–2314.
[21] J.A. Letts, K. Fiedorczuk, L.A. Sazanov, The architecture of respiratory supercomplexes, Nature 537 (2016) 644–648.
[22] J. Gu, et al., The architecture of the mammalian respirasome, Nature 537 (2016) 1–16.
[23] Wu, M., Gu, J., Guo, R., Huang, Y. & Yang, M. Structure of mammalian respiratory supercomplex I1III2IV1. Cell 167, 1598–1609.e10 (2016).
[24] Guo, R., Zong, S., Wu, M. & Yang, M. Architecture of human mitochondrial respiratory megacomplex I2III2IV2. Cell 1–11 (2017) doi:https://doi.org/10.1016/j.cell.2017.07.050.
[25] M. Protasoni, et al., Respiratory supercomplexes act as a platform for complex III-mediated maturation of human mitochondrial complexes I and IV, EMBO J. 39 (2020) 1–19.
[26] Bundgaard, A., James, A. M., Harbour, M. E., Murphy, M. P. & Fago, A. Stable mitochondrial CICIII 2 supercomplex interactions in reptiles compared to homeothermic vertebrates. J. Exp. Biol. jeb.223776 (2020) doi:https://doi.org/10.1242/jeb.223776.
[27] P. Fernández-Silva, R. Acín-Pérez, E. Fernández-Vizarra, A. Pérez-Martos, J. A. Enriquez, In vivo and in organello analyses of mitochondrial translation, Methods Cell Biol. 80 (2007) 571–588.
[28] C.R. Hackenbrock, S.S. Gupte, Mitochondrial electron transport: the random collision model, in: C.H. Kim (Ed.), Advances in Membrane Biochemistry and Bioenergetics, ©Plenum Press, New York, 1987, pp. 61–62.
[29] D. Keilin, E.F. Hartree, Activity of the cytochrome system in heart muscle preparations, Biochem. J. 41 (1947) 500–502.
[30] A. Barrientos, C. Ugalde, I function, therefore I am: overcoming skepticism about mitochondrial supercomplexes, Cell Metab. 18 (2013) 147–149.
[31] D. Milenkovic, J.N. Blaza, N.G. Larsson, J. Hirst, The enigma of the respiratory chain supercomplex, Cell Metab. 25 (2017) 765–776.
[32] R. Pérez-Pérez, et al., COX7A2L is a mitochondrial complex III binding protein that stabilizes the III2+IV supercomplex without affecting respirasome formation, Cell Rep. 16 (2016) 2387–2398.
[33] C. Greggio, et al., Enhanced respiratory chain supercomplex formation in response to exercise in human skeletal muscle, Cell Metab. 25 (2017) 301–311.

[34] J.A. Letts, L.A. Sazanov, Clarifying the supercomplex: the higher-order organization of the mitochondrial electron transport chain, Nat. Struct. Mol. Biol. 24 (2017) 800–808.
[35] C. García-Poyatos, et al., Scaf1 promotes respiratory supercomplexes and metabolic efficiency in zebrafish, EMBO Rep. 21 (2020), e50287.
[36] Tezze, C. et al. Age-associated loss of OPA1 in muscle impacts muscle mass, metabolic homeostasis, systemic inflammation, and epithelial senescence. Cell Metab. 25, 1374–1389.e6 (2017).
[37] M. Gomez-Velazquez, et al., CTCF counter-regulates cardiomyocyte development and maturation programs in the embryonic heart, PLoS Genet. 13 (2017) 1–25.
[38] J.R. Huertas, S. Al Fazazi, A. Hidalgo-Gutierrez, L.C. López, R.A. Casuso, Antioxidant effect of exercise: exploring the role of the mitochondrial complex I superassembly, Redox Biol. 13 (2017) 477–481.
[39] V. Raimondi, F. Ciccarese, V. Ciminale, Oncogenic pathways and the electron transport chain: a dangeROS liaison, Br. J. Cancer (2020), https://doi.org/10.1038/s41416-019-0651-y.
[40] K.M. Davies, C. Anselmi, I. Wittig, J.D. Faraldo-Gomez, W. Kuhlbrandt, Structure of the yeast F1Fo-ATP synthase dimer and its role in shaping the mitochondrial cristae, Proc. Natl. Acad. Sci. 109 (2012) 13602–13607.
[41] K.M. Davies, B. Daum, Role of cryo-ET in membrane bioenergetics research, Biochem. Soc. Trans. 41 (2013) 1227–1234.
[42] T. Stephan, A. Roesch, D. Riedel, S. Jakobs, Live-cell STED nanoscopy of mitochondrial cristae, Sci. Rep. 9 (2019) 1–6.
[43] Y. Wang, et al., Mitochondrial fatty acid oxidation and the electron transport chain comprise a multifunctional mitochondrial protein complex, J. Biol. Chem. 294 (2019) 12380–12391.
[44] B. Muster, et al., Respiratory chain complexes in dynamic mitochondria display a patchy distribution in life cells, PLoS One 5 (2010).
[45] V. Wilkens, W. Kohl, K. Busch, Restricted diffusion of OXPHOS complexes in dynamic mitochondria delays their exchange between cristae and engenders a transitory mosaic distribution, J. Cell Sci. 126 (2013) 103–116.
[46] K.B. Busch, Inner mitochondrial membrane compartmentalization: dynamics across scales, Int. J. Biochem. Cell Biol. 120 (2020) 105694.